iConclusions https://iconclusions.com/ Conclusions in Engineering

Theoretical analysis of power-law nanofluid across extended sheet with thermal-concentration slip and Soret/Dufour effect

Irfan Haider,[1] Imtiaz Ahmad Khan,[1] Fatima Kainat,[1] Hassan Ali Akhtar,[2] Hassaan Khalid,[1] Nawishta Jabeen,[3] and Ahmad Hussain[1, a)]

[1)] *Department of Physics, The University of Lahore, Sargodha campus, 40100 Sargodha, Pakistan*

[2)] *Department of Physics, RIPHAH International University Islamabad, 46200 Islamabad, Pakistan*

[3)] *Department of Physics, Fatima Jinnah Women University Rawalpindi, 46000 Rawalpindi, Pakistan*

ABSTRACT: The present research explores the theoretical analysis of power-law nanofluid across extended sheet with thermal-concentration slip and Soret/Dufour effects. Physical problem is converted into non-linear differential equations via similar transformations. The Keller box method has been utilized to solve the non-linear problems. In the nanofluid framework, the Soret/Dufour and magnetic fields are integrated. The Keller Box approach is apply on explanatory algebraic equations with MATLAB software to extract the numerical and graphical results. Physical features such as temperature description, velocity description, and mass distribution are examined in relation to different flow model variables. The findings show that the velocity profile increases with increasing thermal-concentration slip variable while mass concentration rate decreased. It is found that the heart transmission rate and fluid velocity are increased with increasing Brownian motion and Lewis variable. Present study is useful for the cooling process in industrial mechanical systems.

Received: 26 November 2024 **Accepted:** 14 January 2025
DOI: https://doi.org/10.71107/4v443468

I. INTRODUCTION

The term "nanofluid" refers to a fluid that made up of nano materials. Small pieces of metallic materials such as carbide atoms, or oxides produced at the nanoscale are known as nanoparticles. Inappropriate liquids, including water and grease, have lower thermal conductivity is known as base liquid. The heat and mass transmission rate can be enhanced by simply adding nanomaterial into base liquid. As a result, employing nanofluids to transfer heat can enhance thermal characteristics. The cooling processes, thermal transfer infrastructure, refrigerators, electrically powered hybrid engines, paper making, and automobile heating and cooling maintenance are just a few of the heat transportation applications that benefit from nanofluids' special qualities. Ullah et al.[1] investigated the impacts of temperature-concentration slipping impacts and external magnetic field on second-grade nanofluid technology with variable density and viscous dissipation along extended surfaces. Ullah et al.[2] examined the heat and mass transmission through magnetohydrodynamic (MHD) power-law nanofluid flow over a movable surface using soret/sufour phenomena and surface heat flux.

Ullah et al.[3] used an accelerated non-conducting wedge surface in an imposed magnetic field to assess the effects of thermal slip and varying viscous on thermal conductivity and magnetic flux. Using a magnetic field orthogonal to the plane of the surface to solve this problem is the main objective of the Ullah et al.[4] research. The MHD convection heat transfer and amplitude challenge of electromagnetic fluid flowing down a horizontal non-magnetized circumferential heating container with decreased gravitational and heat stratification has been numerically simulated. The authors were found that the current density rised with increasing oscillation magnitudes, while the transient skin friction

[a)] Electronic mail: ahmed_00277@yahoo.com

and heat transmission rate exhibit a noticeable oscillation intensity at both $\alpha = \pi/6$ and $\pi/2$ locations. Their research sheds important light on the interactions between electromagnetic forces, heating and solutal dispersion, and boundary conditions which comprehend and maximize the behavior of nanofluids. We expand on their approaches and apply the analysis to the entropy optimization and variable density impacts on magneto Ree-Eyring nanofluid flow with different slip conditions, this work serves as a fundamental framework for our investigation.

The MHD combined convection flow of conducting fluid along vertically magnetic and symmetrical warmed surfaces having slip velocity and thermally slip influences has been simulated numerically and physically by Alharbi et al.[5]. Evaluating the heat transmission and magnetic flux across a symmetric magnetize plate while accounting for thermo and velocity slip impacts was innovation in that work. Ullah et al.[6] examined the viscosity dissipation, temperature-dependent density, thermophoresis, and chemical processes that occur when a nanofluid transfers mass and heat across a magnetized driven surface. Ullah et al.[7] analyzed the impacts of solutal and thermal slip on the flow of boundary layer nanofluids through an accelerated wedge. The authors focused the impact of thermophoresis and Brownian motion is taken into consideration in their research work. Ullah et al.[8] employed the convective boundary circumstances to define heat transmission with an emphasis on the physical relevance of heat production and chemical reactions on Carreau nanofluids. Ullah et al.[9] concentrated on integrating the effects of temperature slip and changing viscous on the generated magnetic gradient and heat flux across a rotating non-conducting disk in a magnetic field. Induced magnetization enhances the effectiveness of thermal equipment to maintain thermal rates in engineering and industrial processes. To enhance the thermal performances of transient nanofluid flow over various forms is examined[10–19].

This work is focused on the study of Soret/Dufour phenomena and the impacts on thermal rate and mass transmission in the power-law nanofluid movement under external magnetic fields with thermal-concentration slip across a stretchable surface. Using the Soret/Dufour effect, the particle flow rises with fluctuations in both concentration and temperature. The Newton–Raphson method is applied on ordinary differential equation to integrate the non-similar physical problem with the bvp4c approach. MATLAB software is used to visualize and quantify the results of the mathematical equations. A MATLAB solver called bvp4c solves boundary value problems (BVPs) using a finite difference code. It can deal with problems involving singular terms or unknown parameters and solves systems of ordinary differential equations (ODEs) of the form $y' = (x, y)$ on an interval $[a, b]$. It is investigated how different flow model parameters impacted the mass transport, skin friction, heat transfer, fluid concentrations, temperature description, and velocity pattern. Although the authors[20] came to a conclusion regarding thermal and mass transfer of power-law nanofluids within boundaries, this study uses the Keller box modeling to improve the efficiency and effectiveness of the Nusselt ratio and Sherwood factor by examining the effects of Soret/Dufour on power-law nanofluids along thermal-concentration slip. Following are the key objective of the present study;

1. To investigate the mass and heat transmission in magneto power-law nanofluids over a stretched sheet with multiple slip efect.
2. To examine the Soret/Dufour effect on heat and mass transmission in power-law nanofluid along stretching surface with thermal and cioncentration slip effect.
3. To investigate the magnetic fields effect on mass-heat transmission with flow stability of the nanofluid.

II. PHYSICAL MODEL

This research explores the theoretical analysis of power-law nanofluid across extended sheet with thermal-concentration slip and Soret/Dufour effects with linear velocity, $u_w(x) = Bx$. The refractive index of present model is n, and the surface temperature of extending plate is T_f with variable thermal rate exchanger coefficient $\mathrm{h}(x) = A(1-x)^{1/1+n}$.

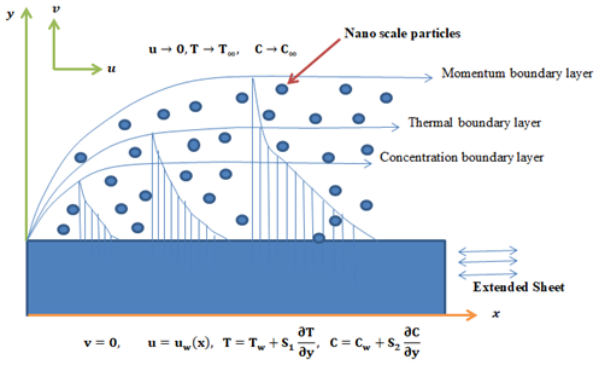

FIG. 1: Extended Sheet for Power-law Nanofluid.

Figure 1 is the model diagram which is demonstrated the non-Newtonian nanofluid flow along extended sheet with horizontal velocity u and vertical velocity v. When dealing with fluids that possess non-Newtonian characteristics, the power law nanofluid model is utilized, which establish the relationship between the ratios of stress and strain as;

$$\tau_{xy} = \mu \left| \frac{\partial u}{\partial y} \right|^{n-1} \frac{\partial u}{\partial y} \tag{1}$$

The partial differential of current model is provided below by the[1,2,20]

$$\frac{\partial u}{\partial x} + \frac{\partial u}{\partial y} = 0 \tag{2}$$

$$u\frac{\partial u}{\partial x} + v\frac{\partial u}{\partial y} = v\frac{\partial}{\partial y}\left[\frac{\partial u}{\partial y}\right]^{n} + \sigma\frac{\mathrm{B}^2\mathbf{0}}{\rho}\mathrm{u} \tag{3}$$

$$\mathrm{u}\frac{\partial T}{\partial x} + v\frac{\partial T}{\partial y} = \alpha\left[\frac{\partial^2 T}{\partial y^2}\right] + \tau\left\{D_B\left(\frac{\partial C}{\partial y}\frac{\partial T}{\partial y}\right) + \frac{D_T}{T_\infty}\left[\frac{\partial T}{\partial y}\right]^2\right\} + \frac{D_{K_T}}{C_s C_p}\frac{\partial^2 C}{\partial y^2} \tag{4}$$

$$u\frac{\partial C}{\partial x} + v\frac{\partial C}{\partial y} = D_B\left(\frac{\partial^2 C}{\partial y^2}\right) + \frac{D_T}{T_\infty}\left(\frac{\partial^2 T}{\partial y^2}\right) + \left(\frac{D_{K_T}}{T_m}\right)\left(\frac{\partial^2 T}{\partial y^2}\right) \tag{5}$$

The boundary condition of present model is

$$v = 0, u = u_w(x), T = T_w + S_1\frac{\partial T}{\partial v}, \quad C = C_w + S_2\frac{\partial C}{\partial v} \text{ at } y = 0 \tag{6}$$

$$u \to 0, T \to T_\infty, \quad C \to C_\infty \quad \text{as} \quad y \to \infty$$

Using following similarity variables by following Khan and Gorla[20]

$$\eta = \left(\frac{B^{2-n}x^{1-n}}{v}\right)^{\frac{1}{(1+n)}} y, \quad \psi = \left(vB^{2n-1}x^{2n}\right)^{\frac{1}{(n+1)}} \mathrm{f}(\eta)$$
$$\theta(\eta) = \frac{T - T_\infty}{T_f - T_\infty}, \quad \phi(\eta) = \frac{C - C_\infty}{C_w - C_\infty} \tag{7}$$

Here ψ is expressed the stream function and it is defined as $u = \frac{\partial \psi}{\partial y}$ and $v = -\frac{\partial \psi}{\partial x}$, here u and v are the

horizontal and vertical component of velocity and given as:

$$V = -\left(vB^{2n-1}x^{n-1}\right)^{\frac{1}{(1+n)}}\left\{\left(\frac{2n}{1+n}\right)\cdot f+\left(\frac{1-n}{1+n}\right)\cdot \eta f'\right\} \tag{8}$$

By applying similarity variables on equation[3–5], it is transformed into following ordinary differential equations:

$$n\left(f''\right)^{n-1}f'''+\left(\frac{2n}{n+1}\right)ff''-f''^2+Mf'=0 \tag{9}$$

$$\frac{1}{Pr}\theta''+\left(\frac{2n}{1+n}\right)f\theta'+Nb\theta'\phi'+Nt\theta'^2+Df\phi'=0 \tag{10}$$

$$\frac{1}{Le}\phi''+\left(\frac{2n}{1+n}\right)\phi' f+\left[\frac{Nt}{Nb}\frac{1}{Le}+Sr\right]\theta''=0 \tag{11}$$

The boundary condition for newly formed ordinary differential equation will be;

$$\begin{gathered} f(0)=0,\quad f'(0)=-\lambda,\theta(0)-S_1\theta'(0)=1,\quad \phi(0)-S_2\phi'(0)=1 \text{ at } \eta=0 \\ f'(\infty)\to 1,\quad \theta(\infty)\to 0,\phi(\infty)\to 0 \quad \text{at } \eta\to\infty \end{gathered} \tag{12}$$

S_1 and S_2 are the thermal and concentration slip factor, magnetic parameter $M=\frac{\sigma {B_0}^2}{\rho B}, Nb = \tau D_B\left(C_w-C_\infty\right)\left[\frac{v^2B^{3(n-1)}x^{2(1-n)}}{\alpha^{1+n}}\right]^{1/1+n}$ is the Brownian factor, $Nt=\frac{\tau D_T(T_w-T_\infty)}{T_\infty}\left[\frac{v^2B^{3(n-1)}x^{2(1-n)}}{\alpha^{1+n}}\right]^{1/1+n}$, $S_r=\frac{DK_T}{T_m}\left(\frac{T_w-T_\infty}{c_w-C_\infty}\right)\left(\frac{B^{3(1-n)}x^{2(1-n)}}{v^2}\right)^{1/1+n}$, $D_f=\frac{DK_T}{C_sC_p}\frac{(C_w-C_\infty)}{(T_w-T_\infty)}\left[\frac{B^{3(1-n)}x^{2(1-n)}}{v^2}\right]^{\frac{1}{1+n}}$ is the value of Dufour parameter, $H_c=\frac{A}{k}\left(\frac{B^{2-n}}{v}\right)^{\frac{1}{1+n}}$, the value of generalized Lewis parameter is $Le=\frac{v}{D_B}\left[\frac{B^{3(n-1)}x^{2(1-n)}}{v^2}\right]^{1/1+n}$, $\mathrm{Pr}=\left[\frac{v^2B^{3(n-1)}x^{2(1-n)}}{\alpha^{1+n}}\right]^{\frac{1}{1+n}}$ and $R=\frac{1+n}{2n}\left[vB^{2n-1}x^{2n-1}\right]^{-\left(\frac{1}{n+1}\right)}V_n$ is the suction/injection parameter.

The values of Sherwood, skin friction and Nusselt number are expressed as:

$$Re_x^{-1/1+n}Sh=-\phi'(0), Re_x^{1/1+n}C_f=2, Re_x^{-1/1+n}Nu=-\theta'(0) \tag{13}$$

The Reynolds factor can be determined as

$$Re_x=\frac{x^n(Bx)^{2-n}}{v} \tag{14}$$

The Sherwood factor ${Re_x}^{-1/(1+n)}Nu_x$ is reducing and the Nusselt factor ${Re_x}^{-1/1+n}\ Sh_x$ is also reduced for present model.

III. MATHEMATICAL APPROACH

We compute these mathematical problems computationally using the Keller Box method and iterative approaches. First, we use $(v)\eta, (\mathrm{p})\eta$ and $(\mathrm{q})\eta$ as independent parameters.

We put

$$\begin{gathered} \theta'=u,\quad \theta''=u',\quad \phi'=l,\quad \phi''=l' \\ f'=p,\quad f''=p' \quad , \quad p'=q,\quad f'''=q' \end{gathered} \tag{15}$$

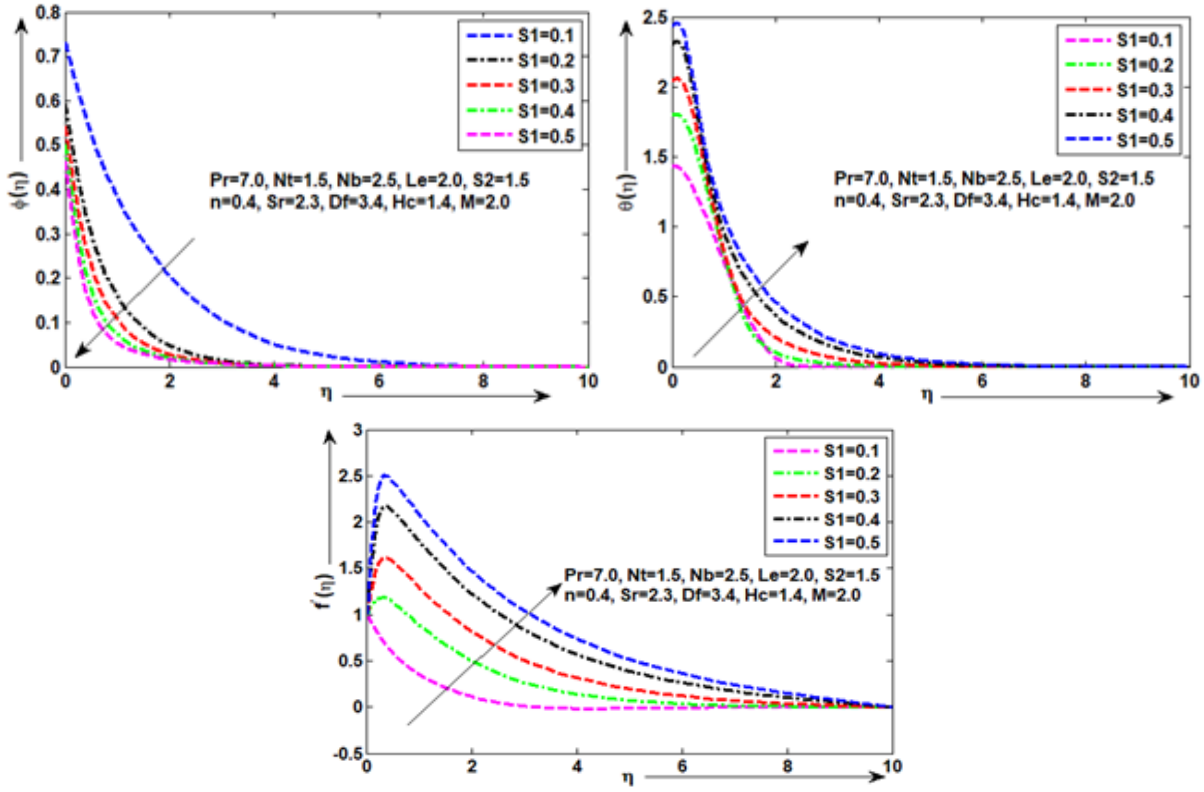

FIG. 2: demonstrates the concentration, thermal and velocity rate for S_1.

The boundary condition is newly formed and for above equation will become:

$$\begin{aligned} f=0,\quad p=-\lambda,\quad \theta-S_1u=1,\\ \phi-S_2l=1\quad \text{at } \eta=0\\ p=1,\quad \theta=0,\phi=0\quad \text{at } \eta\to\infty \end{aligned} \tag{16}$$

The above mentioned equation represented as

$$\begin{aligned} \theta'=u &\Rightarrow \theta'-u=0\\ f'=p &\Rightarrow f'-p=0\\ \phi'=l &\Rightarrow \phi'-l=0\\ p'=q &\Rightarrow p'-q=0 \end{aligned} \tag{17}$$

$$n(q)^{n-1}q'+\left(\frac{2n}{n+1}\right)fq-P^2+MP=0 \tag{18}$$

$$\frac{1}{Pr}u'+\left(\frac{2n}{n+1}\right)fu+Nbul+Ntu^2+Dfl'=0 \tag{19}$$

$$\frac{1}{Le}l'+\left(\frac{2n}{n+1}\right)fl+\left[\frac{Nt}{Nb}\frac{1}{Le}+Sr\right]u'=0 \tag{20}$$

Using central difference methodology on previous mentioned relation;

$$f'=\frac{f_i-f_{i-1}}{h_i}\text{ and }f=\frac{f_i-f_{i-1}}{2}=f_{i-\frac{1}{2}}$$

$$\begin{aligned} \theta_\Omega-\theta_{\Omega-1}-\frac{1}{2}h_\Omega\left(u_\Omega+u_{\Omega-1}\right)=0\\ f_\Omega-f_{\Omega-1}-\frac{1}{2}h_\Omega\left(P_\Omega+P_{\Omega-1}\right)=0\\ \phi_\Omega-\phi_{\Omega-1}-\frac{1}{2}h_\Omega\left(l_\Omega+l_{\Omega-1}\right)=0\\ P_\Omega-P_{\Omega-1}-\frac{1}{2}h_\Omega\left(q_\Omega+q_{\Omega-1}\right)=0 \end{aligned} \tag{21}$$

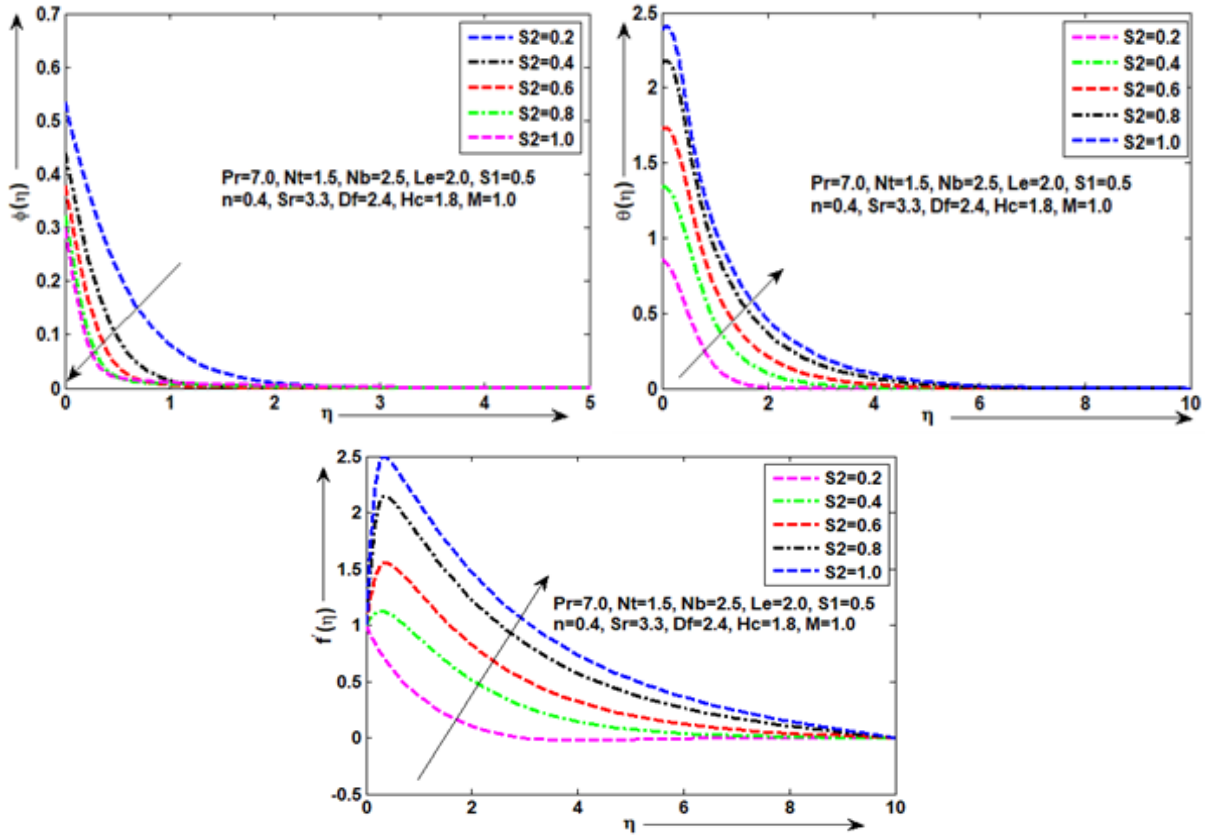

FIG. 3: demonstrates the concentration, thermal and velocity rate for S_1.

$$\frac{n}{h_\Omega}\left(\frac{q_\Omega+q_{\Omega-1}}{2}\right)^{n-1}(q_\Omega-q_{\Omega-1})+\frac{2n}{n+1}(f_\Omega+f_{\Omega-1})(q_\Omega+q_{\Omega-1})-\frac{1}{4}(P_\Omega+P_{\Omega-1})^2+\frac{M}{2}(P_\Omega+P_{\Omega-1})=0 \quad (22)$$

$$\frac{1}{\mathrm{Prh}_\Omega}(u_\Omega+u_{\Omega-1})+\frac{n}{2(n+1)}(f_\Omega+f_{\Omega-1})(u_\Omega+u_{\Omega-1})\frac{Nb}{4}(u_\Omega+u_{\Omega-1})(l_\Omega+l_{\Omega-1})+\frac{Nt}{4}(u_\Omega+u_{\Omega-1})^2+\frac{Df}{h_\Omega}(l_\Omega-l_{\Omega-1})=0 \quad (23)$$

$$\frac{1}{Leh_\Omega}(l_\Omega-l_{\Omega-1})+\frac{n}{2(n+1)}(f_\Omega+f_{\Omega-1})(l_\Omega+l_{\Omega-1})+\frac{1}{h_\Omega}\left[\frac{Nt}{Nb}\frac{1}{Le}+Sr\right](u_\Omega-u_{\Omega-1})=0 \quad (24)$$

The boundaries equations are listed below

$$\begin{gathered} f(0)=0,\quad p(0)=-\lambda,\\ \theta(0)-S_1u(0)=1,\\ \phi(0)-S_2l(0)=1 \text{ at } \eta=0\\ P_\Omega=0,u_\Omega=0,q_\Omega=0 \text{ at } \eta\to\infty \end{gathered} \quad (25)$$

A. Applying Newton-Raphson method

Apply the Newton-Raphson technique on present problems now.

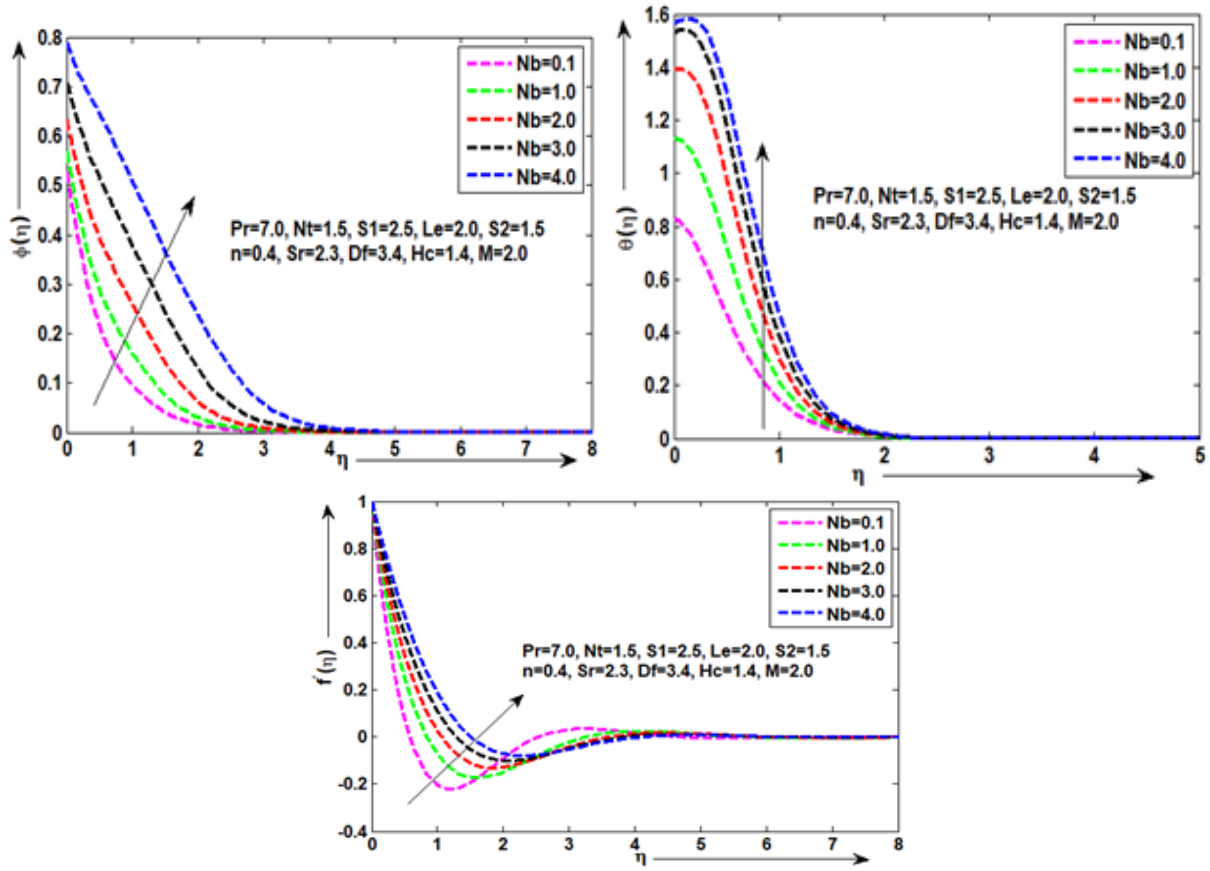

FIG. 4: demonstrates the concentration, thermal and velocity rate for S_1.

$$f_i^{k+1} = f_i^k + \delta f_i^k$$

Where, $i = \Omega$, since we exclude all instances of powers of δ greater than the first power when using the traditional Newton-Raphson technique, the equation becomes

$$\begin{aligned}
\delta\theta_\Omega - \delta\theta_{\Omega-1} - \frac{1}{2}h_\Omega\left(\delta u_\Omega + \delta u_{\Omega-1}\right) &= (r_1)_\Omega \\
\delta f_\Omega - \delta f_{\Omega-1} - \frac{1}{2}h_\Omega\left(\delta P_\Omega + \delta P_{\Omega-1}\right) &= (r_2)_\Omega \\
\delta\phi_\Omega - \delta\phi_{\Omega-1} - \frac{1}{2}h_\Omega\left(\delta l_\Omega + \delta l_{\Omega-1}\right) &= (r_3)_\Omega \\
\delta P_\Omega - \delta P_{\Omega-1} - \frac{1}{2}h_\Omega\left(\delta q_\Omega + \delta q_{\Omega-1}\right) &= (r_4)_\Omega
\end{aligned} \tag{26}$$

$$\begin{aligned}(u_1)\,\delta q_\Omega+(u_2)\,\delta q_{\Omega-1}+(u_3)\,\delta f_\Omega+(u_4)\,\delta f_{\Omega-1}+(u_5)\,\delta P_\Omega+(u_6)\,\delta P_{\Omega-1}&=(r_5)_\Omega\\(v_1)\,\delta q_\Omega+(v_2)\,\delta q_{\Omega-1}+(v_3)\,\delta f_\Omega+(v_4)\,\delta f_{\Omega-1}+(v_5)\,\delta l_\Omega+(v_6)\,\delta l_{\Omega-1}&=(r_6)_\Omega\\(w_1)\,\delta l_\Omega+(w_2)\,\delta l_{\Omega-1}+(w_3)\,\delta f_\Omega+(w_4)\,\delta f_{\Omega-1}+(u_5)\,\delta u_\Omega-(u_6)\,\delta u_{\Omega-1}&=(r_7)_\Omega\end{aligned}\tag{27}$$

The boundary requirements that can be precisely satisfied without iteration are recalled. Consequently, to ensure that these precise values are maintained during each cycle; We can write

$$\begin{gathered}f(0)=0,\quad p(0)=-\lambda,\quad \theta(0)-S_1u(0)=1,\quad \phi(0)-S_2l(0)=1\quad \text{at } \eta=0\\P_\Omega=0,u_\Omega=0,q_\Omega=0\quad \text{at } \eta\to\infty\end{gathered}\tag{28}$$

B. Matrix form

The procedures will either fail because the matrix solving technique needs the presence of a similar matrix including a sub matrix, or it will become exceedingly unfavorable since the matrix includes any discernable structure. This makes it a crucial step.

$$A\delta=r$$

That is

$$\begin{bmatrix}[A_1]\,[C_1] & & & \\ [B_2]\,[A_2]\,[C_2] & & & \\ & \ddots & & \\ & \ddots & & \\ & & [B_{\Omega-1}]\,[A_{\Omega-1}]\,[C_{\Omega-1}] & \\ & & [B_\Omega]\,[A_\Omega] & \end{bmatrix}\begin{bmatrix}[\delta_1]\\[\delta_2]\\[\delta_3]\\\vdots\\[\delta_{\Omega-1}]\\[\delta_\Omega]\end{bmatrix}=\begin{bmatrix}[r_1]\\[r_2]\\[r_3]\\\vdots\\[r_{\Omega-1}]\\[r_\Omega]\end{bmatrix}\tag{29}$$

IV. RESULTS AND DISCUSSION

In this study, the power law magneto-nanofluids across an extended surface with thermal-concentration slip was examined with respect to both mass and heat transport effects. Using a similarity transformation with non-similar formulation, the nonlinear PDEs sre converted into ODEs for present nanofluid model. A computation integration of the final non-similar problem is performed using the Keller box method. Both numerical and visual representations of the explanatory algebraic equations are provided by the MATLAB software. Physical features such as temperature description (0), velocity description $f'(0)$, and mass distribution $\phi(0)$ are examined in relation to different flow model variables.

Figure 2 is demonstrated the influence of thermal slip effects (S_1 = 0.1, 0.2, 0.3, 0.4, 0.5) on mass concentration rate, thermal rate and nanofluid flow rate while values of remaining physical parameters kept fixed. It is noted that concentration boundary declined with inclining the thermal slip parameter as shown in Figure 2(a). The mass concentration rate is maximum at thermal slip value S_1 =0.1 and further reduced on increasing thermal slip parameter and gain minimum mass concentration rate at thermal slip value $S_1 = 0.5$. In many researches it is observed that the mass concentration rate rises with increasing thermal slip parameter but in present model it decreases due to stretching surface. Thermal boundary layer thickness increases with increase in thermal slip factor as shown in Figure 2(b). The thermal rate is minimum at thermal slip parameter value $S_1 = 0.1$ and further increases on increasing thermal slip parameter

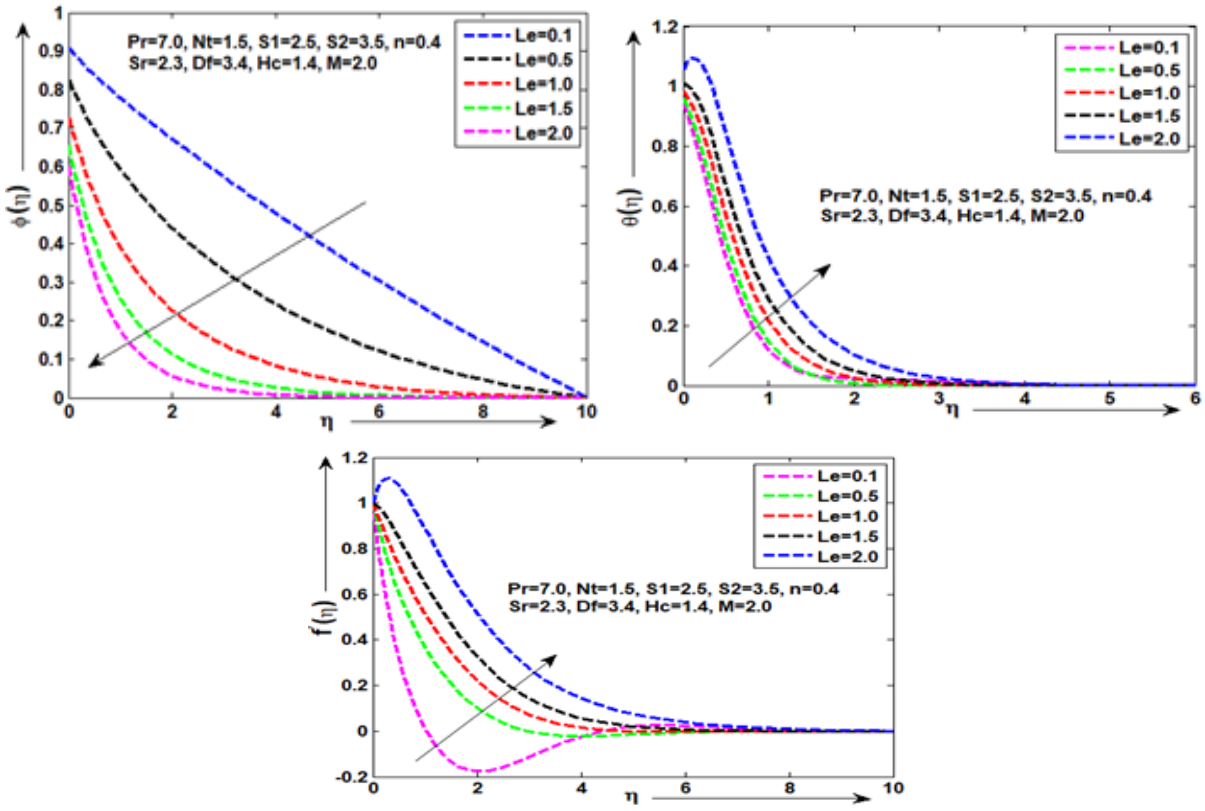

FIG. 5: demonstrates the concentration, thermal and velocity rate for S_1.

and gain maximum thermal rate at $S_1 = 0.5$. The thermal slip variable affects the dimensionless heat transmission rate and it is dependent on the particular flow conditions as well as the characteristics of the fluid and solid surface. Slip effects, which occur when fluids do not follow accros boundaries. It has a variety of uses including conserving energy, friction reducing, and smoothing inside chambers and valves within the heart. The Figure 2(c) shows that the velocity rate rises up with rising the value of thermal slip parameter and attain maximum value at S1=0.5 and minimum value is to be noted at lower values of thermal slip parameter while keeping the value of remaining physical parameter constant.

Figure 3(a-c) demonstrates the influence of concentration slip effects ($S_2 = 0.2, 0.4, 0.6, 0.8, 1.0$) on mass concentration rate, thermal transfer rate and fluid flow rate keeping the values of remaining physical parameters kept fixed. It is noted that concentration boundary declined with inclining concentration slip as shown in Figure 3(a). The mass concentration rate is maximum at S_2 =0.2 and further reduced on increasing concentration slip parameter and gain minimum mass concentration rate at S_2 =2.0. Thermal boundary layer thickness increases with increasing concentration slip factor as shown in Figure 3(b). The thermal transmission rate is minimum at S_2 =0.2 and further increases on increasing concentration slip parameter and gain maximum thermal transmission rate at S_2 =2.0. The Figure 3(c) showed that the velocity rate rise up with rising the value of concentration slip parameter and attain maximum value at S_2 =1.0 and minimum value is to be noted at lower value of concentration slip parameter while keeping the values of remaining physical parameters constant.

The impact of Brownian motion variable (Nb=0.1, 1.0, 2.0, 3.0, 4.0) on mass concentration profile, profile, heat transmission profile and velocity profile are demonstrated in Figured 4(a-c). It is noted that all these three profile (mass concentration profile, heat transmission profile, velocity profile) are increased with increasing Brownian motion variable and get maximum value at Nb=4.0. The Figure 5(a-c) expresses the effect of Lewis variable (Le=0.1, 0.5, 1.0, 1.5, 2.0) on mass transmission rate, heat flow rate and velocity of flowing fluid while

TABLE I: Theoretical values of $f''(0), -\theta'(0)$ and $\phi'(0)$ for $\mathrm{Sr} = 1.0, 2.0, 4.0, 6.0, 7.0$.

Sr	$-f''(0)$	$-\theta'(0)$	$-\phi'(0)$
0.2	1.923977881112351	0.135069252774694	0.494191831370841
0.4	1.701344237532651	0.084864213790988	1.276572068067135
0.8	1.683396363093730	0.036848075388725	1.956767526577293
1.0	1.635151891187262	0.020755287281812	2.496832437333638
1.2	1.609442144543882	0.015858050231376	2.841961059071488

TABLE II: Comparison the values of Pr for $-\theta'(0)$ with published results.

Pr	Noghrehabadi et al.[21]	Abbas et al.[22]	Ullah et al.[1]	Present results
0.07	0.065565	0.065554	0.065554	0.065554
0.02	0.169089	0.169071	0.169069	0.169069
0.7	0.453916	0.453921	0.453920	0.443920
2	0.911358	0.911332	0.911330	0.911330
10	1.895404	1.895456	1.895454	1.885454

keeping the value of other physical factor constant as shown graphically. It is found that the mass transfer rate in nanofluid achieved maximum rate at lower value of Le=0.1 and rate further decreases on increasing Lewis variable as shown in Figure 5a. It is noticed that heat transfer rate and velocity of fluid speed up as we increases the Lewis variable and maximum rate achieved at Le=2.0.

The impact of several Soret number values (Sr = 0.2, 0.4, 0.8, 1.0, 1.2) on skin rate, Nusselt number and Sherwood rate are shown in Table I. After adjusting the other factors, this data may be used to determine how physical factors like mass transmission, skin friction, and heat transmission behave. According to Table I, skin friction reduces at higher value of Soret number (Sr = 1.2) and increases at lower Soret (Sr = 0.2) values. Furthermore, the mass transmission rate is minimum at a very small value of Soret number (Sr = 0.2) and reach its highest value at an even higher percentage of Soret number (Sr = 1.2). The Table II demonstrates the validation of present results with literature.

V. CONCLUSION

A computational model is built to investigate the power-law nanofluid performance along extended surface with thermal-concentration slip conditions and uniform surface nanoparticle concentration. A comparable solution is created by adjusting temperature and Soret/Dufour parameters that are connected to the concentration of the nanofluid. The relationship of skin friction $-f''(0)$, local Nusselt number $-\theta'(0)$, and Sherwood numbers $-\phi'(0)$ is investigated numerically. The velocity profile, temperature profile and mass transmission profile for thermal slip parameter (S_1), concentration slip parameter (S_2) and Brownian motion are found. Following are the principal results.

- The velocity rate are inclined up for higher values of thermal and concentration slip at $S_1 = 0.5$ and $S_2 = 1.2$.
- The mass concentration profile are increased at higher value of thermal and concentration slip at $\mathrm{S}_1 = 0.5$ and $\mathrm{S}_2 = 1.2$ respectively.
- The graphical results are showed that the mass transfer rate is achieved maximum value at lower value of Brownian motion variable.
- It is found that the heart transmission rate and fluid velocity are increased with increasing Brownian motion and Lewis variable.
- The thermal profile is increased at lower values of both thermal-concentration slip at $\mathrm{S}_1 = 0.1$ and $\mathrm{S}_2 = 0.2$ but reduced at higher values.
- The Sherwood profile is increased with increasing prandtl number while the skin friction and Nusselt number are showed reverse effect.

The variable density, activation energy and Hall current effect can be apply on power-law nanofluid to investigate the heat-mass characteristics in future.

DECLARATION OF COMPETING INTEREST

The authors declare that they have no known competing financial interests or personal relationships that could have appeared to influence the work reported in this paper.

ACKNOWLEDGMENTS

The authors are thankful to University of Lahore, Pakistan for ORIC-SRGP 17/2024 research fund to support this research work.

REFERENCES

[1] Z. Ullah, M. M. Alam, J. Younis, I. Haider, M. S. Alqurashi, H. Abu-Zinadah, F. Albouchi, and A. A. Faqihi, "Entropy optimization of mhd second-grade nanofluid thermal transmission along stretched sheet with variable density and thermal-concentration slip effects," Case Studies in Thermal Engineering , 105288 (2024).

[2] Z. Ullah, M. M. Alam, J. Younis, S. H. Elhag, A. Hussain, and I. Haider, "Computational study of heat and mass transfer with soret/dufour effects on power-law magneto nanofluid flow along stretching surface," AIP Advances **14** (2024), 10.1063/5.0134567.

[3] Z. Ullah, H. Alotaibi, A. Usman, I. Khan, and A. S. Omer, "Thermal slip and variable viscosity analysis on heat rate and magnetic flux through accelerating non-conducting wedge in the presence of induced magnetic field," Scientific Reports **14**, 19434 (2024).

[4] Z. Ullah, N. Jabeen, and M. U. Khan, "Amplitude and phase angle of oscillatory heat transfer and current density along a nonconducting cylinder with reduced gravity and thermal stratification effects," Mathematics **11**, 2134 (2023).

[5] K. A. M. Alharbi, Z. Ullah, N. Jabeen, and M. Ashraf, "Magnetohydrodynamic and thermal performance of electrically conducting fluid along the symmetrical and vertical magnetic plate with thermal slip and velocity slip effects," Symmetry **15**, 1148 (2023).

[6] Z. Ullah, A. Hussain, M. S. Aldhabani, N. H. Altaweel, and S. Shahab, "Significance of temperature-dependent density on dissipative and reactive flows of nanofluid along magnetically driven sheet and applications in machining and lubrications," Lubricants **11**, 410 (2023).

[7] Z. Ullah, M. M. Alam, S. H. Elhag, F. E. Merga, I. Haider, and A. Malik, "Evaluation of thermal and concentration slip effects on heat and mass transmission of nanofluid over a moving wedge surface using keller box scheme," AIP Advances **14** (2024), 10.1063/5.0145678.

[8] Z. Ullah, M. M. Alam, U. Tariq, Y. M. Mahrous, F. E. Merga, F. Albouchi, and A. A. Faqihi, "Variable density and heat generation impact on chemically reactive carreau nanofluid heat-mass transfer over stretching sheet with convective heat condition," Case Studies in Thermal Engineering , 105260 (2024).

[9] Z. Ullah, H. Alotaibi, A. Usman, I. Khan, and A. S. Omer, "Thermal slip and variable viscosity analysis on heat rate and magnetic flux through accelerating non-conducting wedge in the presence of induced magnetic field," Scientific Reports **14**, 19434 (2024).

[10] M. Almheidat, Z. Ullah, M. M. Alam, M. Boujelbene, A. Ebaid, M. D. Alsulami, and A. O. Ibrahim, "Entropy generation analysis of oscillatory magnetized darcian flow of mixed thermal convection and mass transfer with joule heat over radiative sheet," Case Studies in Thermal Engineering **61**, 104921 (2024).

[11] Z. Ullah, M. M. Alam, J. Younis, Y. M. Mahrous, F. Albouchi, M. D. Alsulami, and I. Haider, "Thermal conductivity impact on mhd convective heat transfer over moving wedge with surface heat flux and high magnetic prandtl number," Case Studies in Thermal Engineering **61**, 105077 (2024).

[12] Z. Ullah, E. R. El-Zahar, L. F. Seddek, N. Becheikh, B. M. Alshammari, M. S. Aldhabani, and L. Kolsi, "Solar radiation and heat sink impact on fluctuating mixed convective flow and heat rate of darcian nanofluid: Applications in electronic cooling systems," Case Studies in Thermal Engineering **59**, 104592 (2024).

[13] Z. Ullah, "Thermal and concentration slip analysis on heat and mass transfer in magnetic-driven dissipative nanofluid across stretched sheet for high temperature difference," Arabian Journal for Science and Engineering , 1–13 (2024).

[14] I. Boukholda, Z. Ullah, Y. M. Mahrous, A. Alamer, M. B. Amara, M. D. Alsulami, and N. B. Khedher, "Analysis of thermal density and heat sink on dissipative nanofluid along magnetized sheet and applications in microelectronic cooling systems," Case Studies in Thermal Engineering **55**, 104185 (2024).

[15] H. Al-Shammari, Z. Ullah, Y. M. Mahrous, M. S. Aldhabani, M. A. Said, S. Al Arni, and N. B. Khedher, "Arrhenius activation energy and thermal radiation effects on oscillatory heat-mass transfer of darcy forchheimer nanofluid along heat generating cone," Case Studies in Thermal Engineering **57**, 104294 (2024).

[16] Z. Ullah, N. H. Altaweel, M. S. Aldhabani, K. Ghachem, M. Alhadri, and L. Kolsi, "Oscillatory behavior of heat transfer and magnetic flux of electrically conductive fluid flow along magnetized cylinder with variable surface temperature," Mathematics **11**, 3045 (2023).

[17] K. A. M. Alharbi, Z. Ullah, N. Jabeen, and M. Ashraf, "Magnetohydrodynamic and thermal performance of electrically conducting fluid along the symmetrical and vertical magnetic plate with thermal slip and velocity slip effects," Symmetry **15**, 1148 (2023).

[18] Z. Ullah and M. Alkinidri, "Oscillatory and transient role of heat transfer and magnetic flux around magnetic-driven stretching cylinder under convective boundary conditions," Case Studies in Thermal Engineering **50**, 103514 (2023).

[19] Z. Ullah and M. Alkinidri, "Effect of variable viscosity on oscillatory heat and mass transfer in mixed convective flow with chemical reaction along inclined heated plate under reduced gravity," Alexandria Engineering Journal **77**, 539–552 (2023).

[20] W. A. Khan and R. S. Reddy Gorla, "Heat and mass transfer in power-law nanofluids over a nonisothermal stretching wall with convective boundary condition," (2012), dOI not available.

[21] A. Noghrehabadi, M. Ghalambaz, and A. Ghanbarzadeh, "Heat transfer of magnetohydrodynamic viscous nanofluids over an isothermal stretching sheet," Journal of Thermophysics and Heat Transfer **26**, 686–689 (2012).

[22] A. Abbas, A. Hussanan, Z. Ullah, E. R. El-Zahar, and L. F. Seddek, "Heat and mass transfer in magnetohydrodynamic boundary layer flow of second-grade nanofluid fluid past inclined stretching permeable surface implanted in a porous medium," International Journal of Modelling and Simulation , 1–15 (2024).